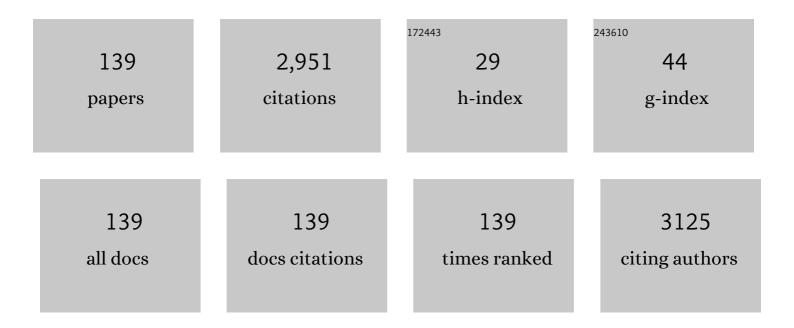
Bai-Wang Sun

List of Publications by Year in descending order

Source: https://exaly.com/author-pdf/856013/publications.pdf Version: 2024-02-01



RALMANC SUN

#	Article	IF	CITATIONS
1	Activatable autophagy inhibition-primed chemodynamic therapy via targeted sandwich-like two-dimensional nanosheets. Chemical Engineering Journal, 2022, 431, 133470.	12.7	17
2	Novel WO ₃ -PEDOT core–shell inverse opal films with enhanced electrochromic performance for smart windows. Functional Materials Letters, 2022, 15, .	1.2	1
3	MOF-shielded and glucose-responsive ultrasmall silver nano-factory for highly-efficient anticancer and antibacterial therapy. Chemical Engineering Journal, 2021, 416, 127610.	12.7	14
4	One-for-all intelligent core–shell nanoparticles for tumor-specific photothermal–chemodynamic synergistic therapy. Biomaterials Science, 2021, 9, 1020-1033.	5.4	32
5	A polydopamine-gated biodegradable cascade nanoreactor for pH-triggered and photothermal-enhanced tumor-specific nanocatalytic therapy. Nanoscale, 2021, 13, 15677-15688.	5.6	14
6	Dual catalytic cascaded nanoplatform for photo/chemodynamic/starvation synergistic therapy. Colloids and Surfaces B: Biointerfaces, 2021, 199, 111538.	5.0	20
7	Small-Molecule-Selective Organosilica Nanoreactors for Copper-Catalyzed Azide–Alkyne Cycloaddition Reactions in Cellular and Living Systems. Nano Letters, 2021, 21, 3401-3409.	9.1	19
8	Three new co-crystals of 2,3,5,6-tetramethyl pyrazin with different substituted aromatic compounds _ crystal structure, spectroscopy and Hirshfeld analysis. Journal of Molecular Structure, 2021, 1241, 130580.	3.6	3
9	A novel pH-responsive Fe-MOF system for enhanced cancer treatment mediated by the Fenton reaction. New Journal of Chemistry, 2021, 45, 3271-3279.	2.8	12
10	Enhanced antitumor effect via amplified oxidative stress by near-infrared light-responsive and folate-targeted nanoplatform. Nanotechnology, 2021, 32, 035102.	2.6	4
11	Glutathione-triggered nanoplatform for chemodynamic/metal-ion therapy. Journal of Materials Chemistry B, 2021, 9, 9413-9422.	5.8	16
12	The solubilities of benzoic acid and its nitro-derivatives, 3-nitro and 3,5-dinitrobenzoic acids. Journal of Chemical Research, 2021, 45, 1100-1106.	1.3	5
13	Multimodal therapies: glucose oxidase-triggered tumor starvation-induced synergism with enhanced chemodynamic therapy and chemotherapy. New Journal of Chemistry, 2020, 44, 1524-1536.	2.8	22
14	Hypoxia-augmented and photothermally-enhanced ferroptotic therapy with high specificity and efficiency. Journal of Materials Chemistry B, 2020, 8, 78-87.	5.8	34
15	Dopamine-assisted synthesis of rGO@NiPd@NC sandwich structure for highly efficient hydrogen evolution reaction. Journal of Solid State Electrochemistry, 2020, 24, 137-144.	2.5	5
16	Biomimetic Platinum Nanozyme Immobilized on 2D Metal–Organic Frameworks for Mitochondrion-Targeting and Oxygen Self-Supply Photodynamic Therapy. ACS Applied Materials & Interfaces, 2020, 12, 1963-1972.	8.0	104
17	Ultra-thin two-dimensional nanosheets for in-situ NIR light-triggered fluorescence enhancement. FlatChem, 2020, 24, 100193.	5.6	10
18	Smart Porous Core–Shell Cuprous Oxide Nanocatalyst with High Biocompatibility for Acidâ€Triggered Chemo/Chemodynamic Synergistic Therapy. Small, 2020, 16, e2001805.	10.0	109

#	Article	IF	CITATIONS
19	A pH-activated autocatalytic nanoreactor for self-boosting Fenton-like chemodynamic therapy. Nanoscale, 2020, 12, 17319-17331.	5.6	58
20	Mesoporous Silica-Coated Silver Nanoframes as Drug-Delivery Vehicles for Chemo/Starvation/Metal Ion Multimodality Therapy. Langmuir, 2020, 36, 6345-6351.	3.5	12
21	Build 3D Nanoparticles by Using Ultrathin 2D MOF Nanosheets for NIR Light-Triggered Molecular Switching. ACS Applied Materials & Interfaces, 2020, 12, 15573-15578.	8.0	16
22	A CD44-targeted Cu(<scp>ii</scp>) delivery 2D nanoplatform for sensitized disulfiram chemotherapy to triple-negative breast cancer. Nanoscale, 2020, 12, 8139-8146.	5.6	24
23	Photothermal-reinforced and glutathione-triggered in Situ cascaded nanocatalytic therapy. Journal of Controlled Release, 2020, 321, 734-743.	9.9	76
24	A novel versatile yolk-shell nanosystem based on NIR-elevated drug release and GSH depletion-enhanced Fenton-like reaction for synergistic cancer therapy. Colloids and Surfaces B: Biointerfaces, 2020, 189, 110810.	5.0	43
25	Dendritic Mesoporous Organosilica Nanoparticles: A pH-Triggered Autocatalytic Fenton Reaction System with Self-supplied H ₂ O ₂ for Generation of High Levels of Reactive Oxygen Species. Langmuir, 2020, 36, 5262-5270.	3.5	18
26	A co-crystal strategy for the solidification of liquid pyrazine derivatives: X-ray structures and Hirshfeld surface analyses. Journal of Molecular Structure, 2020, 1218, 128505.	3.6	2
27	Cisplatin and Ce6 loaded polyaniline nanoparticles: An efficient near-infrared light mediated synergistic therapeutic agent. Materials Science and Engineering C, 2019, 95, 183-191.	7.3	12
28	Three new cocrystals derived from liquid pyrazine spices: X-ray structures and Hirshfeld surface analyses. Research on Chemical Intermediates, 2019, 45, 5745-5760.	2.7	6
29	Enhanced Reactive Oxygen Species Levels by an Active Benzothiazole Complex-Mediated Fenton Reaction for Highly Effective Antitumor Therapy. Molecular Pharmaceutics, 2019, 16, 4929-4939.	4.6	10
30	Porphyrin-Based Hydrogen-Bonded Organic Frameworks for the Photocatalytic Degradation of 9,10-Diphenylanthracene. ACS Applied Nano Materials, 2019, 2, 7719-7727.	5.0	42
31	Photothermal-Enhanced Inactivation of Glutathione Peroxidase for Ferroptosis Sensitized by an Autophagy Promotor. ACS Applied Materials & Interfaces, 2019, 11, 42988-42997.	8.0	75
32	Reactive oxygen species mediated theranostics using a Fenton reaction activable lipo-polymersome. Journal of Materials Chemistry B, 2019, 7, 314-323.	5.8	33
33	Ultralarge Dielectric Relaxation and Self-Recovery Triggered by Hydrogen-Bonded Polar Components. ACS Applied Materials & Interfaces, 2019, 11, 7272-7279.	8.0	20
34	Molecular Disorder Induced by the Application of an External Magnetic Field during Crystal Growth. Journal of Physical Chemistry C, 2019, 123, 15230-15235.	3.1	1
35	Unraveling the Mechanisms of the Excited‣tate Intermolecular Proton Transfer (ESPT) for a Dâ€Ï€â€A Molecular Architecture. Chemistry - A European Journal, 2019, 25, 8805-8812.	3.3	10
36	Enhanced cellular uptake of near-infrared triggered targeted nanoparticles by cell-penetrating peptide TAT for combined chemo/photothermal/photodynamic therapy. Materials Science and Engineering C, 2019, 103, 109738.	7.3	28

#	Article	IF	CITATIONS
37	A novel pH-responsive hollow mesoporous silica nanoparticle (HMSN) system encapsulating doxorubicin (DOX) and glucose oxidase (GOX) for potential cancer treatment. Journal of Materials Chemistry B, 2019, 7, 3291-3302.	5.8	51
38	Atomically Thin Nanoribbons by Exfoliation of Hydrogen-Bonded Organic Frameworks for Drug Delivery. ACS Applied Nano Materials, 2019, 2, 2437-2445.	5.0	52
39	Ultrathin two-dimensional nanosheets meet upconverting nanoparticles: <i>in situ</i> near-infrared triggered molecular switching. Journal of Materials Chemistry C, 2019, 7, 3965-3972.	5.5	16
40	Porous High-Valence Metal–Organic Framework Featuring Open Coordination Sites for Effective Water Adsorption. Inorganic Chemistry, 2019, 58, 3058-3064.	4.0	22
41	Three peroxidovanadium(<scp>v</scp>) compounds mediated by transition metal cations for enhanced anticancer activity. Dalton Transactions, 2019, 48, 15160-15169.	3.3	5
42	Sulfosalicylic acid/Fe ³⁺ based nanoscale coordination polymers for effective cancer therapy by the Fenton reaction: an inspiration for understanding the role of aspirin in the prevention of cancer. Biomaterials Science, 2019, 7, 5482-5491.	5.4	17
43	A small-sized and stable 2D metal–organic framework: a functional nanoplatform for effective photodynamic therapy. Dalton Transactions, 2019, 48, 16861-16868.	3.3	17
44	The antitumor activity of 4,4â \in 2-bipyridinium amphiphiles. RSC Advances, 2019, 9, 33023-33028.	3.6	2
45	Enhanced treatment effect of nanoparticles containing cisplatin and a GSH-reactive probe compound. Materials Science and Engineering C, 2019, 96, 635-641.	7.3	3
46	Mesoporous silica-coated gold nanoframes as drug delivery system for remotely controllable chemo-photothermal combination therapy. Colloids and Surfaces B: Biointerfaces, 2019, 176, 230-238.	5.0	28
47	A novel near-infrared triggered dual-targeted nanoplatform for mitochondrial combined photothermal-chemotherapy of cancer <i>in vitro</i> . Nanotechnology, 2019, 30, 035601.	2.6	19
48	Comparison Between the Acidification of Acidic and Alkalic Groups. Crystal Growth and Design, 2019, 19, 437-443.	3.0	10
49	Two-dimensional metal organic framework for effective gas absorption. Inorganic Chemistry Communication, 2019, 101, 27-31.	3.9	12
50	pH and thermo dual stimulus-responsive liposome nanoparticles for targeted delivery of platinum-acridine hybrid agent. Life Sciences, 2019, 217, 41-48.	4.3	18
51	1,3-dimethyl-6-nitroacridine derivatives induce apoptosis in human breast cancer cells by targeting DNA. Drug Development and Industrial Pharmacy, 2019, 45, 212-221.	2.0	4
52	Binding CO ₂ from Air by a Bulky Organometallic Cation Containing Primary Amines. ACS Applied Materials & Interfaces, 2018, 10, 9495-9502.	8.0	35
53	Bidirectional Photoswitching via Alternating NIR and UV Irradiation on a Core–Shell UCNP–SCO Nanosphere. ACS Applied Materials & Interfaces, 2018, 10, 16666-16673.	8.0	34
54	A dual-targeting strategy for enhanced drug delivery and synergistic therapy based on thermosensitive nanoparticles. Journal of Biomaterials Science, Polymer Edition, 2018, 29, 1360-1374.	3.5	11

#	Article	IF	CITATIONS
55	Thermal-Induced Dielectric Switching with 40K Wide Hysteresis Loop Near Room Temperature. Journal of Physical Chemistry Letters, 2018, 9, 2158-2163.	4.6	45
56	Delivery of coumarin-containing all-trans retinoic acid derivatives via targeted nanoparticles encapsulating indocyanine green for chemo/photothermal/photodynamic therapy of breast cancer. New Journal of Chemistry, 2018, 42, 8805-8814.	2.8	10
57	FA and cRGD dual modified lipid-polymer nanoparticles encapsulating polyaniline and cisplatin for highly effective chemo-photothermal combination therapy. Journal of Biomaterials Science, Polymer Edition, 2018, 29, 397-411.	3.5	22
58	Confinement of Reagents in Crystalline Matrix with the Help of Magnetic Field. ChemistrySelect, 2018, 3, 71-76.	1.5	7
59	3-Nitroacridine derivatives arrest cell cycle at G0/G1 phase and induce apoptosis in human breast cancer cells may act as DNA-target anticancer agents. Life Sciences, 2018, 206, 1-9.	4.3	21
60	N-donor ligands-directed coordination of Zn- azido complexes. Inorganica Chimica Acta, 2018, 469, 424-430.	2.4	6
61	The length of ankyl chain tuning the structure and properties of organic assemblies composed of triazole and organic acids. Journal of Molecular Structure, 2018, 1153, 96-105.	3.6	4
62	Co-delivery of cisplatin and CJM-126 via photothermal conversion nanoparticles for enhanced synergistic antitumor efficacy. Nanotechnology, 2018, 29, 015601.	2.6	14
63	Subcellular co-delivery of two different site-oriented payloads based on multistage targeted polymeric nanoparticles for enhanced cancer therapy. Journal of Materials Chemistry B, 2018, 6, 6752-6766.	5.8	21
64	Atomically Thin Two-Dimensional Nanosheets with Tunable Spin-Crossover Properties. Journal of Physical Chemistry Letters, 2018, 9, 7052-7058.	4.6	29
65	A Dynamic 3D Hydrogenâ€Bonded Organic Frameworks with Highly Water Affinity. Advanced Functional Materials, 2018, 28, 1804822.	14.9	80
66	Decoration of Cisplatin on 2D Metal–Organic Frameworks for Enhanced Anticancer Effects through Highly Increased Reactive Oxygen Species Generation. ACS Applied Materials & Interfaces, 2018, 10, 30930-30935.	8.0	85
67	NIR stimulus-responsive core–shell type nanoparticles based on photothermal conversion for enhanced antitumor efficacy through chemo-photothermal therapy. Nanotechnology, 2018, 29, 285302.	2.6	18
68	Iron Oxide Nanocarrier-Mediated Combination Therapy of Cisplatin and Artemisinin for Combating Drug Resistance through Highly Increased Toxic Reactive Oxygen Species Generation. ACS Applied Bio Materials, 2018, 1, 270-280.	4.6	36
69	Tuning the crystal structures of metal-tetraphenylporphines <i>via</i> a magnetic field. New Journal of Chemistry, 2018, 42, 12570-12575.	2.8	6
70	Synthesis and biological evaluation of redox/NIR dual stimulus-responsive polymeric nanoparticles for targeted delivery of cisplatin. Materials Science and Engineering C, 2018, 92, 453-462.	7.3	25
71	Single-Layered Two-Dimensional Metal–Organic Framework Nanosheets as an in Situ Visual Test Paper for Solvents. ACS Applied Materials & Interfaces, 2018, 10, 28860-28867.	8.0	64
72	pH-sensitive prodrug conjugated polydopamine for NIR-triggered synergistic chemo-photothermal therapy. European Journal of Pharmaceutics and Biopharmaceutics, 2018, 128, 260-271.	4.3	33

#	Article	IF	CITATIONS
73	Enhanced highly toxic reactive oxygen species levels from iron oxide core–shell mesoporous silica nanocarrier-mediated Fenton reactions for cancer therapy. Journal of Materials Chemistry B, 2018, 6, 5876-5887.	5.8	59
74	Assembly of 6-aminonicotinic acid and inorganic anions into different dimensionalities: Crystal structure, absorption properties and Hirshfeld surface analysis. Polyhedron, 2017, 124, 243-250.	2.2	10
75	Folate-modified, indocyanine green-loaded lipid-polymer hybrid nanoparticles for targeted delivery of cisplatin. Journal of Biomaterials Science, Polymer Edition, 2017, 28, 690-702.	3.5	39
76	A strategy for photothermal conversion of polymeric nanoparticles by polyaniline for smart control of targeted drug delivery. Nanotechnology, 2017, 28, 165102.	2.6	28
77	Nearâ€Infrared Light and pH Dualâ€Responsive Targeted Drug Carrier Based on Coreâ€Crosslinked Polyaniline Nanoparticles for Intracellular Delivery of Cisplatin. Chemistry - A European Journal, 2017, 23, 5352-5360.	3.3	46
78	Effect of halogen bonding on supramolecular assembly and photophysical properties of diaryl oxalates. Structural Chemistry, 2017, 28, 1731-1742.	2.0	2
79	Tuning the structures and photophysical properties of 9,10-distyrylanthrance (DSA) via fluorine substitution. New Journal of Chemistry, 2017, 41, 4220-4233.	2.8	14
80	Compatibility study of rivaroxaban and its pharmaceutical excipients. Journal of Thermal Analysis and Calorimetry, 2017, 130, 1569-1573.	3.6	17
81	Identification of novel 3-nitroacridines as autophagy inducers in gastric cancer cells. New Journal of Chemistry, 2017, 41, 4087-4095.	2.8	0
82	Enhanced legumain-recognition and NIR controlled released of cisplatin-indocyanine nanosphere against gastric carcinoma. European Journal of Pharmacology, 2017, 794, 184-192.	3.5	11
83	Protonation-induced color change of an amino group functionalized [Fe 4 (μ 3 -O) 2] 8+ cluster. Dyes and Pigments, 2017, 143, 239-244.	3.7	18
84	Selective separation of aqueous sulphate anions via crystallization of sulphate–water clusters. CrystEngComm, 2017, 19, 3362-3369.	2.6	9
85	Reversibly Stretching Cocrystals by the Application of a Magnetic Field. Crystal Growth and Design, 2017, 17, 2576-2583.	3.0	19
86	A series of enzyme-controlled-release polymer-platinum-based drug conjugates for the treatment of gastric cancer. European Polymer Journal, 2017, 92, 105-116.	5.4	4
87	A Twoâ€Dimensional Supramolecular Ice Layer Containing "Quasi hair―(H ₂ 0) ₆ Hexagons Templated by Organic Carboxylic Host. ChemistrySelect, 2017, 2, 61-64.	1.5	15
88	Enhanced cytotoxicity by a benzothiazole-containing cisplatin derivative in breast cancer cells. New Journal of Chemistry, 2017, 41, 773-785.	2.8	18
89	Folate-decorated and NIR-activated nanoparticles based on platinum(IV) prodrugs for targeted therapy of ovarian cancer. Journal of Microencapsulation, 2017, 34, 675-686.	2.8	17
90	Complexation of different transition metals with 4-(4-carboxyphenyl)-1,2,4-triazole: Synthesis, crystal structure and hirshfeld surfaces. Journal of Molecular Structure, 2017, 1149, 136-141.	3.6	2

#	Article	IF	CITATIONS
91	Halogen-bonding contacts determining the crystal structure and fluorescence properties of organic salts. New Journal of Chemistry, 2017, 41, 9444-9452.	2.8	4
92	Substituent swap affects the crystal structure and properties of N-benzyl-4-amino-1,2,4-triazole related organic salts. New Journal of Chemistry, 2017, 41, 13846-13854.	2.8	1
93	Anionsâ€Mediated Morphological Control of Nano―/Microscaled Materials: A Case Study of Protonated Melamineâ€Based Selfâ€Assemblies. ChemistrySelect, 2017, 2, 10505-10511.	1.5	2
94	Near infrared radiated stimulus-responsive liposomes based on photothermal conversion as drug carriers for co-delivery of CJM126 and cisplatin. Materials Science and Engineering C, 2017, 80, 362-370.	7.3	29
95	Two complexes of copper (II) and cobalt (II) with N,O-chelating heterocyclic carboxylates: Crystal structures, Hirshfeld surfaces, and thermal properties. Inorganic and Nano-Metal Chemistry, 2017, 47, 493-499.	1.6	2
96	Co-crystallization of a benzimidazole derivative with carboxylic acids. Research on Chemical Intermediates, 2017, 43, 817-828.	2.7	2
97	Influence of chlorine substitution on the crystal structures of diaryl oxalate. Research on Chemical Intermediates, 2017, 43, 1591-1607.	2.7	0
98	Study of spin crossover in an iron(II) tris(diimine) system tuned by counter anions. Polyhedron, 2017, 121, 101-106.	2.2	20
99	Identification of novel small molecule Beclin 1 mimetics activating autophagy. Oncotarget, 2017, 8, 51355-51369.	1.8	12
100	Lanthanide-based coordination compounds based on 4-(4-carboxyphenyl)-1,2,4-triazole: synthesis, structures, Hirshfeld surface and luminescence properties. New Journal of Chemistry, 2016, 40, 3892-3898.	2.8	9
101	Synthesis, Structural Characterization, and Magnetic Properties of Two Iron(II) Complexes With Triazole- and Imidazole-Related Ligands. Synthesis and Reactivity in Inorganic, Metal Organic, and Nano Metal Chemistry, 2016, 46, 1725-1734.	0.6	0
102	Synthesis, crystal structure, Hirshfeld surface analysis and DNA binding properties of interactions with lattice pyrazinamide and its zinc(II) coordination polymer. Research on Chemical Intermediates, 2016, 42, 6947-6957.	2.7	3
103	Complexation of different transition metals with 4,4′-dimethyl-2,2′-bipyridine: Crystal structure, UV spectra and Hirshfeld surfaces. Spectrochimica Acta - Part A: Molecular and Biomolecular Spectroscopy, 2016, 166, 1-7.	3.9	18
104	Magnetic observation of above room-temperature spin transition in vesicular nano-spheres. Journal of Materials Chemistry C, 2016, 4, 8061-8069.	5.5	50
105	Ambient-Temperature Spin-State Switching Achieved by Protonation of the Amino Group in [Fe(H ₂ Bpz ₂) ₂ (bipy-NH ₂)]. Inorganic Chemistry, 2016, 55, 8147-8152.	4.0	66
106	Influence of Halogen Atoms on Spin rossover Properties of 1,2,4â€Triazoleâ€Based 1D Iron(II) Polymers. ChemistrySelect, 2016, 1, 3879-3884.	1.5	15
107	Counter-anions-tuned crystal structure and intermolecular interactions of a series of iron (II) complexes derived from 4,4′-dimethyl-2,2′-bipyridine. Molecular Crystals and Liquid Crystals, 2016, 631, 132-143.	0.9	1
108	Crystals of 4-(2-benzimidazole)-1,2,4-triazole and its hydrate: preparations, crystal structure and Hirshfeld surfaces analysis. Research on Chemical Intermediates, 2016, 42, 3157-3168.	2.7	45

#	Article	IF	CITATIONS
109	The influence of perchloric acid on 2,3-dimethylpyrazine and 1,2-bis(4-pyridyl)ethane: crystal structure and Hirshfeld surfaces analysis. Research on Chemical Intermediates, 2016, 42, 673-685.	2.7	1
110	Quantitative comparisons between α, β, γ, and δ pyrazinamide (PZA) polymorphs. Research on Chemical Intermediates, 2015, 41, 7059-7072.	2.7	21
111	Effective Laboratory-Scale Preparation of Axitinib by Two Cul-Catalyzed Coupling Reactions. Organic Process Research and Development, 2015, 19, 849-857.	2.7	18
112	Biological evaluation of a novel Herceptin-platinum (II) conjugate for efficient and cancer cell specific delivery. Biomedicine and Pharmacotherapy, 2015, 73, 116-122.	5.6	12
113	Study of stability and drug-excipient compatibility of estradiol and pharmaceutical excipients. Journal of Thermal Analysis and Calorimetry, 2015, 120, 839-845.	3.6	18
114	Trastuzumab-cisplatin conjugates for targeted delivery of cisplatin to HER2-overexpressing cancer cells. Biomedicine and Pharmacotherapy, 2015, 72, 17-23.	5.6	20
115	Copper-catalyzed intramolecular dehydrogenative cyclization: direct access to sensitive formyl-substituted imidazo[1,2-a]pyridines. RSC Advances, 2015, 5, 93631-93634.	3.6	8
116	Influence of halogen atoms on the structures and photophysical properties of 9,10-distyrylanthracene (DSA). CrystEngComm, 2015, 17, 9228-9239.	2.6	14
117	A new salt of dyclonine (DYC): synthesis, crystal structure, luminescent properties, thermal and biological activities. Research on Chemical Intermediates, 2015, 41, 4021-4029.	2.7	Ο
118	Synthesis, co-crystal structure and characterization of pyrazinamide with m-hydroxybenzoic acid, p-hydroxybenzoic acid and 3,4-dihydroxy benzolic acid. Research on Chemical Intermediates, 2015, 41, 2939-2951.	2.7	15
119	Selection of excipients for dispersible tablets of itraconazole through the application of thermal techniques and Raman spectroscopy. Journal of Thermal Analysis and Calorimetry, 2014, 115, 2391-2400.	3.6	10
120	Crystal structure, Hirshfeld surfaces and DNA cleavage investigation of two copper(II) complexes containing polypyridine and salicylide ligands. Spectrochimica Acta - Part A: Molecular and Biomolecular Spectroscopy, 2014, 126, 81-85.	3.9	5
121	Co-crystallization of pyridine-2-carboxamide with a series of alkyl dicarboxylic acids with different carbon chain: Crystal structure, spectroscopy and Hirshfeld analysis. Spectrochimica Acta - Part A: Molecular and Biomolecular Spectroscopy, 2014, 120, 228-236.	3.9	21
122	Mixed azide and substituted 1,2,4-triazole co-ligand bridged 1D chain cadmium(ii) motif: crystal structure, Hirshfeld surfaces and spectroscopic studies. RSC Advances, 2014, 4, 11698.	3.6	10
123	Supramolecular assembly and host–guest interaction of crown ether with inorganic acid and organic amine containing carboxyl groups. New Journal of Chemistry, 2014, 38, 723-729.	2.8	33
124	Positions of amino groups on ammonium salts tunes the conformations of crown ethers: crystal structures, Hirshfeld surfaces and spectroscopic studies. CrystEngComm, 2014, 16, 5319-5330.	2.6	17
125	Compatibility of medroxyprogesterone acetate and pharmaceutical excipients through thermal and spectroscopy techniques. Journal of Thermal Analysis and Calorimetry, 2014, 117, 731-739.	3.6	7
126	Two new metastable forms of 6-chloroquinolin-2(1H)-one: Crystal structure, Hirshfeld surfaces and spectroscopic studies. Spectrochimica Acta - Part A: Molecular and Biomolecular Spectroscopy, 2014, 120, 381-388.	3.9	13

#	Article	IF	CITATIONS
127	2-Methyl-3-chloro-9-hydroxy-4-oxo-4H-pyrido[1,2-a]pyrimidine Hydrochloride: Crystal Structure and Interaction with DNA. Journal of Chemical Crystallography, 2013, 43, 70-75.	1.1	1
128	An investigation into the substituent effect of halogen atoms on the crystal structures of indole-3-carboxylic acid (ICA). CrystEngComm, 2013, 15, 7490.	2.6	31
129	Monitoring the Crystallization Process of Methylprednisolone Hemisuccinate (MPHS) from Ethanol Solution by Combined ATR-FTIR- FBRM- PVM. Separation Science and Technology, 2013, 48, 1881-1890.	2.5	14
130	Pharmaceutical Co-Crystals of Pyrazinecarboxamide (PZA) with Various Carboxylic Acids: Crystallography, Hirshfeld Surfaces, and Dissolution Study. Crystal Growth and Design, 2013, 13, 2098-2106.	3.0	100
131	Two Novel Salts of Tris(hydroxymethyl)aminomethane (THAM): Synthesis, Crystal Structure, Thermal and Hirshfeld Surfaces Analysis. Journal of Chemical Crystallography, 2013, 43, 576-584.	1.1	8
132	A polymer–drug conjugate for doxorubicin: Synthesis and biological evaluation of pluronic F127â€doxorubicin amide conjugates. Journal of Applied Polymer Science, 2012, 124, 4953-4960.	2.6	4
133	A cocrystal strategy for the precipitation of liquid 2,3-dimethyl pyrazine with hydroxyl substituted benzoic acid and a Hirshfeld surfaces analysis of them. CrystEngComm, 2012, 14, 6860.	2.6	58
134	Syntheses, Crystal Structure and Properties of Two 1-D Coordination Polymers Bridged by Dicyanamides. Journal of Chemical Crystallography, 2012, 42, 628-632.	1.1	19
135	Aquabis(2-methyl-4-oxopyrido[1,2-a]pyrimidin-9-olato)cobalt (II): Crystal Structure and Spectroscopic Properties. Journal of Chemical Crystallography, 2011, 41, 715-720.	1.1	1
136	Synthesis of Yâ€shaped poly(<i>N</i> , <i>N</i> â€dimethylaminoâ€2â€ethyl methacrylate) and poly(trimethylen	e) Ţj ETQq 3.1	0 0 0 rgBT /Ov

137	Three Novel Copper-Radical Complexes: Syntheses, Crystal Structures, and Magnetic Properties. European Journal of Inorganic Chemistry, 2010, 2010, 3506-3512.	2.0	11
138	A novel large Ni-azido circle with tridentate (NNO) Schiff base co-ligands: hexagonal structure and ferromagnetic properties. New Journal of Chemistry, 2010, 34, 190-192.	2.8	12
139	Yâ€shaped poly(ethylene glycol) and poly(trimethylene carbonate) amphiphilic copolymer: Synthesis and for drug delivery. Journal of Polymer Science Part A, 2008, 46, 8131-8140.	2.3	27